SPECTROSCOPY AND REACTION KINETICS OF HS RADICALS *

J.J. TIEE, F.B. WAMPLER, R.C. OLDENBORG and W.W. RICE
Los Alamos National Laboratory, University of California, Los Alamos, New Mexico 87545, USA

Received 23 April 1981

A laser-induced fluorescence technique is used to monitor the HS radical concentration. The rate constants at room temperature have been determined for the reaction of HS radical with various added scavengers.

1. Introduction

Fossil fuels are known to be rich in sulfur deposits so that large amounts of sulfur-containing pollutants such as SO_2 and H_2S are formed upon combustion. Although radicals such as HS and SO are important precursors to these pollutants, very little kinetic information exists for reactions of these radicals. The primary objective of this research is to determine the rate constants and Arrhenius parameters for those reactions of the HS radicals that are of importance in coal combustion chemistry.

In this letter we present our current research effort in developing a laser-induced fluorescence (LIF) diagnostic for HS. The principal advantage of such a technique is that the measurements are made in real time and are not dependent upon the ultimate product formation in which secondary reactions may mask or alter the desired kinetic information. The fact that the sampling process is done with no physical intervention of the reaction system and with a minimal amount of product contamination makes the method extremely attractive.

The strong $A\,^2\Sigma^+ - X\,^2\Pi$ transition of the HS radicals has been studied extensively by many workers using flash photolysis–absorption techniques [1–3] and a chemical excitation–emission technique [4]. Various rotational and vibrational constants of the electronic states were derived. In a recent study of the 193 nm photodissociation of H_2S by Hawkins and Houston [5] a LIF technique similar to that employed here was used for determining the HS internal energy distribution. In their work it was determined that only a small amount of excitation is partitioned into the internal energy of the HS fragments upon photodissociation of H_2S at 193 nm. From this observation, it was inferred that most of the available energy appears in the relative recoil coordinate between the H and HS radicals in agreement with a quasi-diatomic kinematic picture of the dissociation. Our experimental observations yield similar conclusions. It should be noted that in our reaction studies precautions are taken to avoid kinetic complications that were evident under low-pressure conditions due to translationally "hot" species. However, reactions of "hot" species are of interest by their own right and are currently being examined in a separate study.

2. Experimental

With the exception of a few minor modifications, the experimental apparatus is the same as reported in a previous publication [6]. The apparatus will be described only briefly here. The main photodissociation source is a modified Tachisto inert-gas halide excimer laser (ArF at 193 nm) that is used to produce HS via the photolysis of H_2S. The laser is typically operated at 3 Hz with an output energy of 15 mJ (25 ns fwhm). In addition, a CO_2 laser is available if we desire to produce HS via IR multiple photon dis-

---

* Work performed under the auspices of the US Department of Energy.

sociation of selected mercaptans. Either a Molectron UV 24 nitrogen-laser pumped DL-II dye laser or a Chromatix CMX-4 flash-lamp-pumped dye laser is used to monitor the nascent population distribution of the HS photofragments. These dye lasers have a tuning range of 217–700 nm. Despite the relatively long pulse width (0.6 μs fwhm) of the CMX-4 laser, it is preferred because the output energy is two orders of magnitude higher at the desired wavelength and it was presumed at the time that the $^2\Sigma^+$ state of HS has a relatively long natural lifetime (0.55 μs) [7]. However, our recent study on the collision-free lifetime of the $^2\Sigma^+$ states of both HS and DS radicals using a Nd^+ : YAG-laser pumped dye laser is contradictory to the results reported in the literature [7]. Our results indicate that the collision-free fluorescence lifetime of the ground vibrational manifold of the HS $^2\Sigma^+$ state ($\leqslant$10 ns) is much shorter than the reported value [7]. We will present these findings in more detail in a later publication.

All lasers with the exception of the CO_2 laser are mildly focused into the cell. They are aligned to overlap spatially throughout the middle portion of the reaction cell observation zone and are fired with various adjustable time delays. The detection system, which is situated perpendicular to the laser beams, is composed of signal collection optics, band pass filters, a $\frac{1}{4}$ m monochromator, and a thermoelectrically cooled PMT (RCA C31034). The fluorescence signal is then processed with the use of boxcar averagers and a chart recorder for spectral scanning. A fast photodiode (RCA 935) is also used for detecting the dye laser pulse. Spectral scanning is accomplished by rationing the LIF signal to that of the dye laser in order to compensate for the variation in dye laser output energy present during second-harmonic tuning. In addition, transient digitizers and a minicomputer are used for temporal studies and signal-averaging experiments. Subroutines are written to program the computer to evaluate the kinetic rates from a given set of LIF data.

The H_2S used is of the highest purity available from commercial sources (Scientific Gas Products, Inc., 99.995%), and the O_2, Ar, NO and C_2H_4 used are research grade products from Matheson Gas Products. They were used without further purification. The gas mixtures (H_2S; Ar) are premixed in a large ballast tank (≈30 ℓ) and are then recirculated through the cell chamber to ensure a fresh sample within the observation zone during the course of the experiments. A large amount of Ar buffer gas is added in order to ensure that thermal vibrational–rotational distributions exist within the radicals investigated, and also to avoid gas diffusion problems. All pressures are monitored with various MKS Baratron heads. At present. all experiments are carried out at room temperature. The current experimental arrangement can be easily adapted to include a temperature-controlled furnace for future temperature experiments.

3. Results and discussion

In our initial experiments, an ArF laser and a N_2-laser pumped dye laser were used as the photolysis and the probe lasers, respectively. It was found that only a small amount of LIF signal was observed under high ArF laser fluences ($\geqslant$50 mJ/cm^2) and high H_2S concentrations (>100 mTorr). This was attributed to the very weak energy of the N_2-laser pumped dye laser in the wavelength region of interest (320–330 nm). Most of the observed signal was believed to be from S_2 emission which severely masked the desired HS fluorescence. This was determined by the prominent S_2 band heads observed in the 320–330 nm region and the short lifetime component of the emission (≈35 ns for S_2 in this spectral region as compared to ≈0.5 μs for HS). The fact that increasing the Ar buffer gas concentration resulted in a large enhancement of the LIF signal and that the fluorescence intensity reached a maximum microseconds after the onset of the photolysis laser indicated that the majority of the signal was due to secondary kinetic processes. It was then decided that in order to do "clean" kinetic studies both the ArF laser fluence and the concentration of the parent molecular species had to be lowered to avoid secondary processes such as secondary photolysis and radical–radical reactions. This can be accomplished if a stronger probe laser is used since the dye laser was far from saturating the HS transition. Therefore, a flash-lamp-pumped dye laser (CMX-4) which was capable of producing a few hundred μJ in the spectral region of interest was employed. Even though such a laser produced a relatively long pulse (≈0.6 μs), it was found to be quite adequate for making kinetic

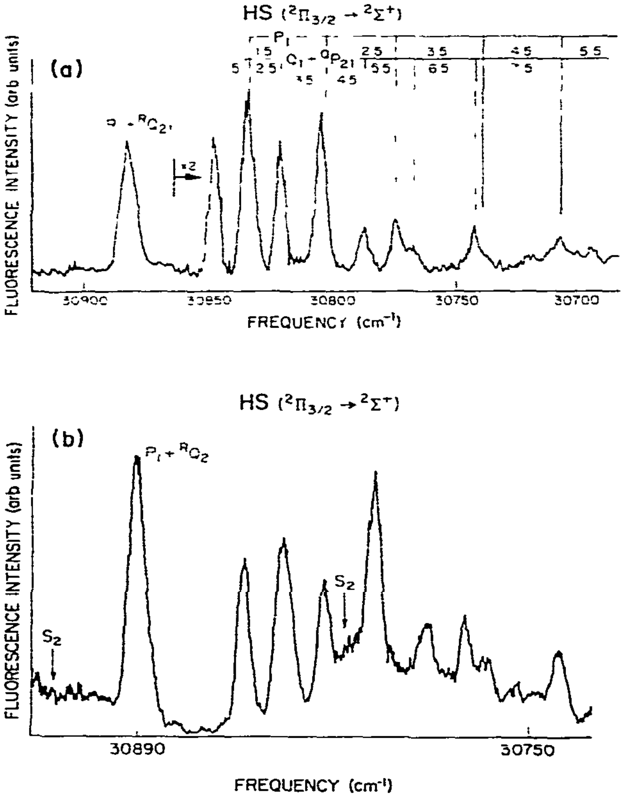

Fig. 1. Fluorescence excitation spectrum of the $^2\Pi_{3/2}$–$^2\Sigma^+$ transition of the HS radicals with a delay time of (a) 1 μs and (b) 50 μs between the two lasers.

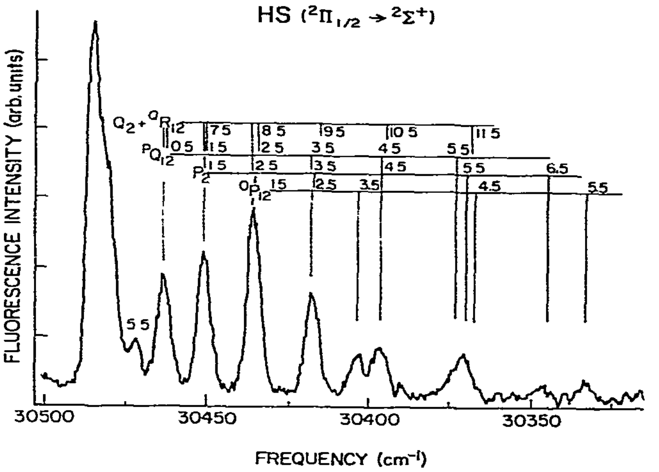

Fig. 2. Fluorescence excitation spectrum of the $^2\Pi_{1/2}$–$^2\Sigma^+$ transition of the HS radicals with a delay time of 1 μs between the two lasers.

measurements of a species such as HS which is reasonably long lived.

Fig. 1a shows the excitation fluorescence spectrum in the region of 323.6–325.7 nm recorded for 30 mTorr of H_2S and 5 Torr of Ar with a delay time of 1 μs between the two lasers. This was done by fixing the detection system with band-pass filters and tuning the probe laser. All peaks are identified to correspond to rotational transitions of the (0, 0) band of the $^2\Pi_{3/2} \rightarrow {}^2\Sigma^+$ HS system. No observable background peaks can be assigned to be due to other species. Experiments with long delay times (≈50 μs) were also carried out. Similar results were obtained with the exception that the signal amplitude dropped significantly. However, when the photolysis laser fluence was increased to more than 50 mJ/cm^2, small S_2 fluorescence peaks started to appear at the long time delays as shown in fig. 1b. By controlling the experimental conditions, clean and unobscured excitation spectra can easily be obtained. Similar results could be observed for the (0, 0) band of the $^2\Pi_{1/2} \rightarrow {}^2\Sigma^+$ system as shown in fig. 2. In examining the (1, 1) band of the same $^2\Pi \rightarrow {}^2\Sigma^+$ transition, no LIF signal was observed. This is indicative of the fact that a very small amount of excess energy is funneled into the internal degrees of freedom of the photofragments upon photodissociation of H_2S as reported by Hawkins and Houston [5].

Fig. 3 depicts the emission spectrum of the HS radicals when excited by the probe laser tuned to the (0, 0) $R_1 + {}^RQ_{21}$ band head. In fig. 3a one sees the emission from both the (0, 0) and (0, 1) bands, the doublets being the $^2\Pi_{3/2}$ and $^2\Pi_{1/2}$ states. The difference in amplitude between the two vibronic bands reflects solely the variation in their Franck–Condon factors. The spectra in figs. 3b and 3c show the same scans over the 320–334 nm and 352–364 nm regions with a higher spectral resolution (≈0.25 nm). The rotational structure of each band head is clearly visible and all spectral features were identified as HS transitions. Again, all spectra indicate that the detection method can be entirely free of background species. It clearly demonstrates that the LIF scheme can be used to completely fingerprint the HS radicals spectrally and can undoubtedly be employed as a useful diagnostic tool.

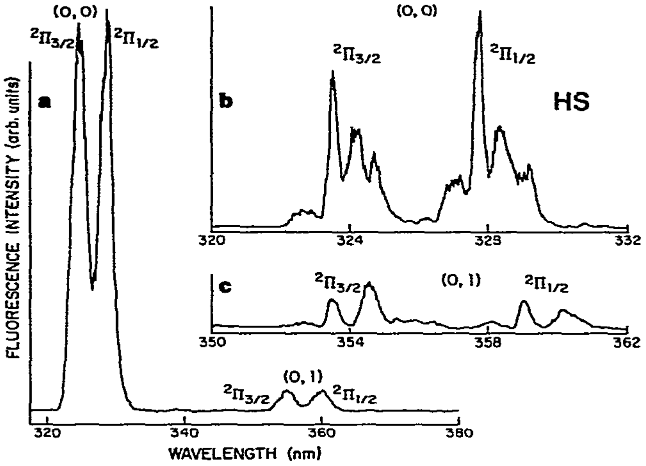

Fig. 3. Emission spectrum of the HS radicals when excited by the dye laser tuned to the $R_1 + {}^RQ_{21}$ band head of the (0, 0) $^2\Pi_{3/2}$–$^2\Sigma^+$ transition.

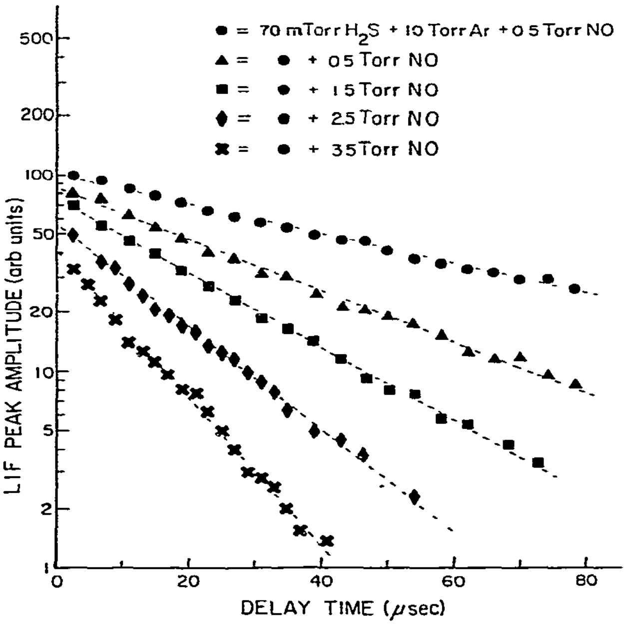

Fig. 4. A semilog plot of the normalized LIF peak amplitude as a function of the delay time for various concentrations of NO.

Fig. 4 shows one such measurement of the disappearance of the HS radicals in NO with 10 Torr of argon added. The HS radicals are produced by the photolysis of 50 mTorr of H_2S by ArF photons and are monitored via LIF by exciting the (0, 0) of the $A\,^2\Sigma^+$–$X\,^2\Pi_{3/2}$ transition near 323.6 nm. The LIF signal is proportional to the concentration of the ground-state HS molecules. The LIF peak amplitude is plotted against the time delay between the two lasers on a semilog graph. With the assumption of pseudo-first-order reaction kinetics, the rate constant for the reaction can be obtained by finding the slope of the plot that is obtained by replotting the lifetime information as a function of the reactive gas concentration. This is shown in fig. 5. A rate constant of 5.6×10^{-13} cm³/molecule s is measured.

As for the measurement of the slower reactive species such as O_2 and C_2H_4, the simple pseudo-first-order kinetic modeling becomes increasingly inadequate, for the fast radical–radical, radical–molecule reactions such as $H + HS \rightarrow H_2 + S$, $HS + HS \rightarrow H_2S + S$, and $H + H_2S \rightarrow H_2 + HS$ start to play relatively more dominant roles. Third body type reactions such as

$$HS + HS\ (H) \xrightarrow{M} H_2S_2\ (H_2S)$$

and

$$H + O_2 \xrightarrow{M} HO_2$$

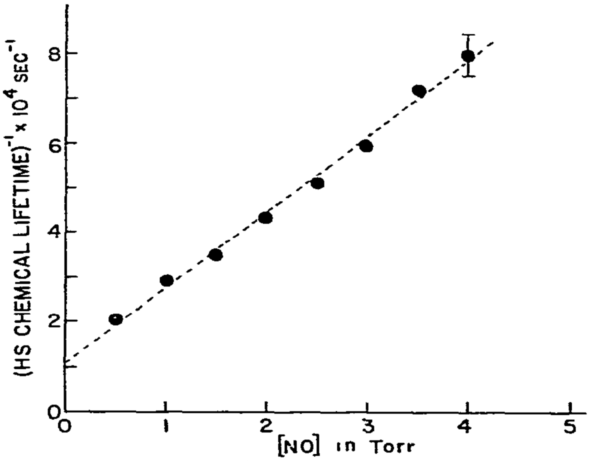

Fig. 5. A plot of the inverse of the HS chemical lifetime as a function of the NO concentration.

become significantly more important as result of large amount of additive gas concentration. This is rather apparent since under high-concentration conditions the HS concentration decay curves deviate from a single exponential. It is found that under many circumstances a $1/x$ functional fit gives a smaller standard deviation. We are currently developing a kinetic code that would take into account all the important reaction parameters. Table 1 presents some of our preliminary measurements for the reaction rate constants of interest. For the slow reactive species only an upper bound of the rate constants is determined. A more precise measurement will be reported when a more complete kinetic code is employed in fitting the data. Product species such as OH and SO are monitored which also provide additional kinetic information.

Table 1
Rate constants at room temperature for HS reactions HS + M

M	(cm^3/molecule s)	(Torr^{-1} s^{-1})
O_2	$<3.2 \times 10^{-15}$	$<9.5 \times 10^{1}$
NO	5.6×10^{-13}	1.7×10^{4}
C_2H_4	$<2.3 \times 10^{-15}$	$<7 \times 10^{1}$
H_2S H HS	$<1.7 \times 10^{-11}$	$<5 \times 10^{5}$

References

[1] M.N. Lewis and J.U. White, Phys. Rev. 55 (1939) 894.
[2] G. Porter, Discussions Faraday Soc. 9 (1950) 60.
[3] D.A. Ramsay, J. Chem. Phys. 20 (1952) 1920.
[4] C.M. Pathak and H.B. Palmer, J. Mol. Spectry. 32 (1969) 157.
[5] W.G. Hawkins and P.L. Houston, J. Chem. Phys. 73 (1980) 297.
[6] J.J. Tiee, F.B. Wampler and W.W. Rice, Chem. Phys. Letters 73 (1980) 519.
[7] K.H. Becker and D. Haaks, J. Photochem. 1 (1972) 177.